



Article

Investigation of Engine Exhaust Heat Recovery Systems Utilizing Thermal Battery Technology

Bo Zhu *, Yi Zhang and Dengping Wang *

School of Automobile and Transportation Engineering, Hefei University of Technology, Hefei 230009, China; zy244346883@163.com

* Correspondence: zhubo@hfut.edu.cn (B.Z.); 2016800218@hfut.edu.cn (D.W.)

Abstract: Over 50% of an engine's energy dissipates via the exhaust and cooling systems, leading to considerable energy loss. Effectively harnessing the waste heat generated by the engine is a critical avenue for enhancing energy efficiency. Traditional exhaust heat recovery systems are limited to real-time recovery of exhaust heat primarily for engine warm-up and fail to fully optimize exhaust heat utilization. This paper introduces a novel exhaust heat recovery system leveraging thermal battery technology, which utilizes phase change materials for both heat storage and reutilization. This innovation significantly minimizes the engine's cold start duration and provides necessary heating for the cabin during start-up. Dynamic models and thermal management system models were constructed. Parameter optimization and calculations for essential components were conducted, and the fidelity of the simulation model was confirmed through experiments conducted under idle warm-up conditions. Four distinct operational modes for engine warm-up are proposed, and strategies for transitioning between these heating modes are established. A simulation analysis was performed across four varying operational scenarios: WLTC, NEDC, 40 km/h, and 80 km/h. The results indicated that the thermal battery-based exhaust heat recovery system notably reduces warm-up time and fuel consumption. In comparison to the cold start mode, the constant speed condition at 40 km/h showcased the most significant reduction in warm-up time, achieving an impressive 22.52% saving; the highest cumulative fuel consumption reduction was observed at a constant speed of 80 km/h, totaling 24.7%. This study offers theoretical foundations for further exploration of thermal management systems in new energy vehicles that incorporate heat storage and reutilization strategies utilizing thermal batteries.

Keywords: thermal management system; thermal battery; engine exhaust heat recovery



Citation: Zhu, B.; Zhang, Y.; Wang, D. Investigation of Engine Exhaust Heat Recovery Systems Utilizing Thermal Battery Technology. *World Electr. Veh. J.* **2024**, *15*, 478. <https://doi.org/10.3390/wevj15100478>

Academic Editor: Joeri Van Mierlo

Received: 23 August 2024

Revised: 5 October 2024

Accepted: 15 October 2024

Published: 21 October 2024



Copyright: © 2024 by the authors. Published by MDPI on behalf of the World Electric Vehicle Association. Licensee MDPI, Basel, Switzerland. This article is an open access article distributed under the terms and conditions of the Creative Commons Attribution (CC BY) license (<https://creativecommons.org/licenses/by/4.0/>).

1. Introduction

The thermal efficiency of gasoline engines ranges from 25% to 35%, whereas diesel engines achieve efficiencies between 35% and 45% [1]. A substantial amount of thermal energy generated from fuel combustion is dissipated into the atmosphere through exhaust gases and the engine's cooling system, leading to considerable energy losses. The recovery and repurposing of this waste heat are crucial for enhancing energy efficiency and minimizing emissions. For instance, automotive heating systems and exhaust gas recirculation (EGR) systems exemplify effective methods of engine waste heat reclaim. The heating system involves channeling heat from the engine into the cabin or onto the windshield via the heating core to elevate cabin temperature or facilitate defrosting. The utilization of heat from the engine's coolant is designated as a water heating system; conversely, harnessing heat from the exhaust system is referred to as air heating [2]. While water heating systems are prevalent, their thermal output tends to be relatively modest, which may result in the engine operating in a supercooled condition during low ambient temperatures. Air heating devices, in contrast, generate substantial heat, offer effective heating results, and exhibit reduced sensitivity to environmental temperature variations, thereby exerting minimal

influence on engine performance. However, it is essential to monitor exhaust back pressure to avoid adverse effects on engine efficiency. The EGR system mitigates the oxygen concentration during combustion by recirculating a portion of the exhaust gas back into the combustion chamber, thus lowering the emission of nitrogen oxides (NO_x). Its primary role is to decrease vehicular exhaust output and enhance combustion efficiency within the engine.

The methods employed to utilize engine waste heat incorporate technologies [3–5] such as thermoelectric power generation, the organic Rankine cycle, and waste heat refrigeration techniques. Thermoelectric power generation [6] harnesses the Seebeck and Peltier effects inherent in semiconductor materials; when a temperature gradient exists across these materials, it produces an electromotive force, enabling the direct conversion of thermal energy into electrical energy. However, due to its relatively low thermoelectric conversion efficiency and high production costs, its practical applications are constrained. The organic Rankine cycle [7] takes advantage of the refrigerant's property of transitioning from liquid to high-pressure vapor upon absorbing engine exhaust heat, which subsequently drives an expansion machine to generate electricity. This technology is currently in the research and development phase. Waste heat refrigeration technology [8] employs the thermal absorption and release properties of absorbents and solvents to achieve cooling of engine waste heat. Presently, lithium bromide solution is predominantly utilized as the absorbent, with water serving as the refrigerant; however, its complex structure makes it ill-suited for vehicles frequently subjected to rough conditions.

The preceding analysis indicates that directly harnessing waste heat from an engine represents a viable technical approach in the short term, particularly concerning the utilization of waste heat from engine cooling water. In recent years, this methodology has expanded to encompass the recovery and utilization of exhaust waste heat, with products starting to penetrate the market [9]. For example, BorgWarner integrates an EGR system with an exhaust heat recovery system (EHRS). During the cold engine starts, the control valve directs the exhaust gas to a heat exchanger, utilizing the thermal energy from the exhaust to heat the engine coolant. This process facilitates rapid engine heating, consequently lowering emissions and enhancing fuel efficiency. Nonetheless, this system is limited to immediate recovery and utilization of exhaust heat and lacks the capability to store and reuse it, resulting in relatively low energy utilization efficiency.

The widespread industrialization of new energy vehicles, particularly hybrid models, necessitates precise engine control in terms of start–stop operations due to the integration of electric drive systems. Extended periods of engine shutdown can result in a drop in temperature upon restart, negatively impacting fuel efficiency and emissions during engine ignition, as well as cabin heating driven by engine coolant. The synergy between the thermal storage properties of phase change materials (PCMs) and EHRSs is emerging as a pivotal trend in the advancement of next-generation thermal management systems for automobiles [10]. This approach effectively leverages PCMs to capture and recycle engine heat, significantly enhancing cold start performance as well as the heating capabilities for both the cabin and battery during cold start scenarios. Furthermore, the retained thermal energy can swiftly elevate the engine temperature during the restart sequence post-shutdown, thereby mitigating fuel consumption and emissions during repeated start–stop cycles.

Pertti Kauranen et al. [11] integrated an EHRS with a latent heat storage component, employing a phase change thermal storage medium of trisodium phosphate dodecahydrate to capture and retain heat insulated by a stainless-steel vacuum vessel. Dheeraj Kishor Johar et al. [12] engineered a cylindrical thermal storage apparatus aimed at harvesting and conserving exhaust heat from internal combustion engines. The device's outer shell is insulated using a combination of glass wool and gypsum, housing 38 small cylinders that encapsulate the erythritol phase change thermal storage material. Four fins encircle the small cylinders to enhance thermal conductivity. Kaltakkiran et al. [13] proposed a thermal energy storage framework that incorporates PCMs primarily designed to store residual

heat from engine coolant in a phase change energy storage context, which can subsequently elevate the intake temperature during cold start scenarios. Under experimental conditions of 6 °C, this approach achieves reductions in cold start cycles and CO and HC emissions by approximately 68.2%, 27.5%, and 44%, respectively, when compared to conventional engine systems. The Fraunhofer Institute for Transport Infrastructure Systems in Germany and Konvekta collaboratively developed a rapid heating and energy storage solution that utilizes a paraffin PCM for swift heating within the cabins of urban electric buses, targeting a cabin temperature of around 18 °C. Soliman et al. [14] devised an energy storage heat exchanger that employs PCMs for waste heat recovery from exhaust gasses, facilitating the preheating of intake temperatures for diesel engines during cold starts. Kraft et al. [15,16] introduced two conceptual designs for energy storage devices utilizing PCMs, one featuring a high-temperature PCM for thermal energy storage and the other incorporating two distinct phase transition temperatures, with a high-temperature PCM situated centrally and a low-temperature PCM located externally, separated by a thermal insulation layer to mitigate heat loss from the thermal storage center. Wang Yongchuan [17] created a cylindrical thermal storage unit featuring 37 concentric sleeves filled with a lithium nitrate phase change thermal storage material aimed at capturing and storing high-temperature exhaust heat from the engine. Experimental tests on an engine bench evaluated fuel consumption and emissions during cold starts, although the considerable size and weight of the thermal storage device compromised its practical application in real vehicles. Yang Qirong [18] investigated the utilization of PCM thermal energy storage spheres to capture waste heat from engine coolant for cold-starting vehicles in low-temperature conditions. Gao Qing [19] selected $\text{Ba}(\text{OH})_2 \cdot 8\text{H}_2\text{O}$ as the PCM for storing and recuperating waste heat from engine coolant, exploring the dynamic phase change process of PCM heat storage through the use of three-dimensional simulations.

The aforementioned literature indicates that researchers have explored the architecture and implications of integrating PCM thermal storage with engine waste heat recovery systems. The predominant focus of this research has been on the recovery and application of waste heat from engine cooling water. In studies addressing the fusion of exhaust heat recovery with PCM thermal storage, the primary emphasis has been on utilizing exhaust waste heat to heat the engine intake, along with assessing the resulting impact on emissions and fuel efficiency. Currently, there is a paucity of research investigating the synergy between engine exhaust waste heat recovery and phase change thermal energy storage, particularly in the context of using recovered waste heat to preheat engine cooling water. This paper investigates an innovative thermal management system for engines based on thermal battery technology, leveraging the thermal storage capabilities of the PCMs within a thermal battery to capture and recycle exhaust heat, thereby significantly enhancing the engine's cold start performance. Thermal battery technology serves as the cornerstone for the forthcoming generation of integrated thermal management systems for new energy vehicles. A thermal management system predicated on thermal battery technology can address challenges related to variances in thermal energy conversion time, spatial considerations, and thermal energy needs, ultimately enabling decoupling and the energy-efficient regulation of thermal management and energy management systems in low-temperature conditions.

2. The Fundamental Design Framework of a Thermal Management System That Utilizes Thermal Battery for the Recovery of Engine Exhaust Heat

A thermal battery represents a specialized form of thermal energy storage system, often referred to as a thermal reservoir [10,20]. The thermal energy retained within can be discharged in a precise and efficient manner, tailored to specific temperature requirements and heat exchange effectiveness. Thermal batteries have well-established industrial applications [21,22], primarily categorized into three dominant technology pathways: water-based thermal storage, solid-state thermal storage, and phase change thermal storage. These systems find utility in photovoltaic heating applications or portable heating solutions, with

their role in the automotive sector predominantly revolving around phase change thermal storage mechanisms [10,23–25].

The configuration of the engine thermal management system, which integrates engine exhaust heat recovery with a thermal battery, is illustrated in Figure 1. The engine exhaust pipe connects to a three-way valve and an exhaust heat exchanger. This three-way valve regulates the exhaust flow either through the heat exchanger or allows for direct discharge. The water circuit of the exhaust heat exchanger links to the engine's small circulation loop, enabling the transfer of exhaust heat to the cooling water for engine heating. The exhaust heat exchanger and thermal battery are connected in parallel within the engine cooling circuit, with control valves RV1 and RV2 managing the operation of their respective circuits. The inlet of the engine cooling water jacket connects to the water pump, while its outlet connects to the thermostat. The thermostat modulates the flow of engine coolant between the small circulation and heat dissipation circuits. Additionally, a radiator is incorporated into the engine cooling circuit. When the engine's water temperature rises excessively, the thermostat directs the coolant to flow through the radiator for cooling purposes. The operation of the radiator and fan must be evaluated comprehensively, considering factors such as vehicle speed and engine water temperature.

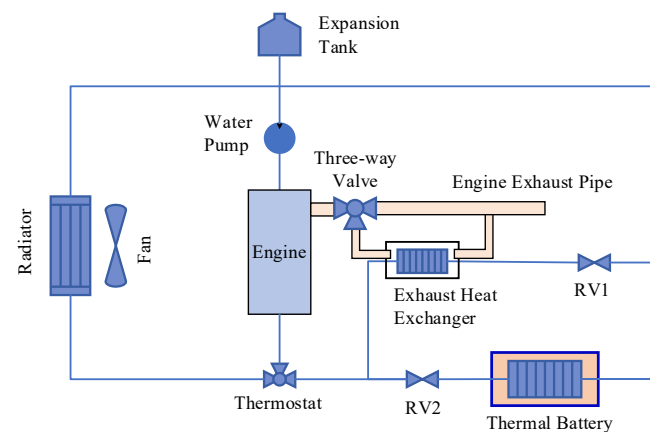


Figure 1. Schematic diagram of the engine exhaust heat recovery system.

Figure 2 presents a schematic illustration of the configuration of the thermal battery. The finned heat exchanger is situated within the thermal battery and is filled with a PCM. The upper section of the thermal battery casing is outfitted with coolant inlets and outlets, which are linked to the corresponding inlet and outlet of the heat exchanger. The coolant circulates through the heat exchanger, facilitating thermal energy exchange with the PCM, thereby enabling the storage or release of thermal energy. To minimize external heat loss from the thermal battery enclosure, insulation material is applied to its exterior surface. The external dimensions of the thermal battery enclosure measure $410 \times 264 \times 65$ mm, while the inlet and outlet diameter of the finned tube heat exchanger is 10 mm.

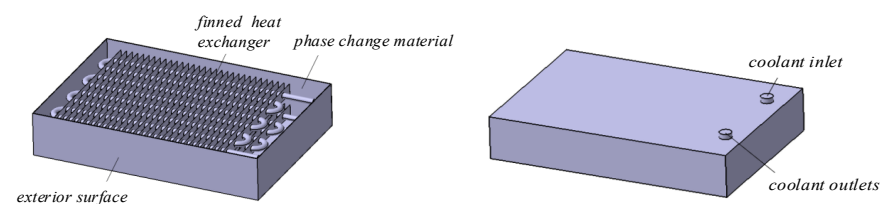


Figure 2. Thermal battery structural diagram.

As an energy storage unit, system efficiency is crucial, and the coefficient of performance (COP) is an indicator used to measure the efficiency of a thermal system. The specific COP can be defined as $COP = \text{useful heat output} / \text{input energy}$. For heat recovery

systems, the COP is typically used to evaluate the ratio between the energy recovered from waste heat and the energy consumed during system operation. The higher the COP, the higher the energy efficiency of the system, which can recover more useful heat from less energy input. The COP of the system is related to factors such as heat transfer efficiency and insulation effect.

Considering the properties of various solid–liquid PCMs and the criteria for engine exhaust heat recovery and coolant heating, $\text{Ba}(\text{OH})_2 \cdot 8\text{H}_2\text{O}$ has been chosen as the thermal energy storage medium for this study. Its characteristic parameters are detailed in Table 1:

Table 1. Characteristic parameters of PCMs.

Phase Change Temperature/ $^{\circ}\text{C}$	Latent Heat/ $\text{kJ}\cdot\text{kg}^{-1}$	Solid Density/ $\text{kg}\cdot\text{m}^{-3}$	Specific Heat Capacity/ $\text{J}/\text{kg}\cdot\text{k}^{-1}$
78	265	2180	1556

The cost of $\text{Ba}(\text{OH})_2 \cdot 8\text{H}_2\text{O}$ is relatively low, especially when compared to other high-performance phase change materials. By combining this material with composites, such as graphite, its thermal conductivity is significantly enhanced, reducing heat loss and improving system efficiency [26]. Experimental results have shown that in solar thermal storage systems, this material exhibits excellent thermal stability, with almost no noticeable energy loss after repeated cycles. This indicates outstanding energy-saving performance during multiple cycles [26]. Moreover, the thermal storage performance of $\text{Ba}(\text{OH})_2 \cdot 8\text{H}_2\text{O}$ can be further enhanced through appropriate material modifications, such as the addition of nucleating agents like BaCl_2 , which helps to reduce supercooling and improve overall system efficiency and economic benefits [27]. Current research has not identified any significant environmental toxicity associated with the use of $\text{Ba}(\text{OH})_2 \cdot 8\text{H}_2\text{O}$. However, it does react with CO_2 in the air to form BaCO_3 , which may lead to material degradation over time. Therefore, proper encapsulation and isolation from air are necessary to ensure the long-term stability of the material [28]. In conclusion, $\text{Ba}(\text{OH})_2 \cdot 8\text{H}_2\text{O}$ shows promise as a phase change material due to its cost-effectiveness and potential for fuel savings.

3. Engine Thermal Management System Model

3.1. Engine Thermal Balance Model

Engine thermal balance [29] pertains to the challenge of distributing the total heat generated from the combustion of fuel within the engine. Typically, a significant proportion of this heat is expelled through exhaust gases and coolant, which represent the primary contributors to engine waste heat. Conducting an energy analysis of engine waste heat involves examining the distribution of energy across various components of the engine in the context of thermal balance. In the thermal equilibrium state, the total heat resulting from fuel combustion is classified into four categories: the heat transformed into effective power for vehicle propulsion, the heat carried away by coolant, the heat expelled via exhaust, and additional heat losses. The thermal equilibrium process unfolds as follows in Equation (1):

$$Q_f = Q_e + Q_w + Q_g + Q_{other} \quad (1)$$

(1) The total heat Q_f :

Based on the engine's fuel consumption rate, the total heat of combustion within the cylinder can be determined using the following Equation (2):

$$Q_f = \frac{B_e H_u}{3600} \quad (2)$$

In Equation (2), B_e represents the fuel consumption of the engine, kg/h; H_u represents the fuel calorific value, which is 44,000 kJ/kg. The calculation formula for the engine's fuel consumption B_e is as follows:

$$B_e = \frac{Q_e b_e}{1000} \quad (3)$$

In Equation (3), Q_e represents the effective power of the engine, kW; b_e signifies the specific fuel consumption rate of the engine, g/(kW·h), obtained through interpolation of engine speed and torque. The detailed fuel consumption MAP is illustrated in Figure 3.

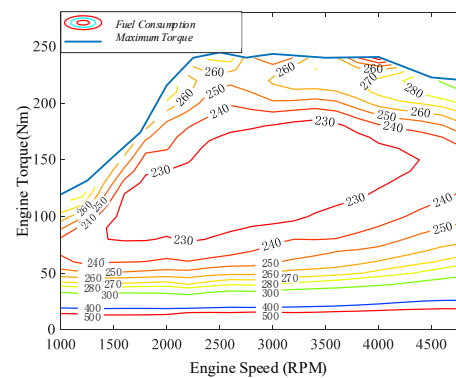


Figure 3. Engine universal characteristic diagram.

(2) Heat converted into effective work Q_e :

$$Q_e = \frac{T_e N_e}{9550} \quad (4)$$

In Equation (4), T_e is the engine torque, Nm; N_e is the engine speed, r/min.

(3) The heat carried away by the engine coolant Q_w :

$$Q_w = C_{w,p} M_w (t_2 - t_1) \quad (5)$$

In Equation (5), $C_{w,p}$ is the constant pressure specific heat capacity of the engine coolant, kJ/(kg·K); M_w is the mass flow rate of the coolant, kg/s; t_1 and t_2 are the inlet and outlet water temperatures of the engine water jacket coolant, K.

(4) Heat carried away by engine exhaust Q_g :

The composition of engine exhaust is complex, and the temperature and pressure of engine exhaust vary greatly under different operating conditions. Therefore, the heat of the engine exhaust is a difficult point in the calculation of the engine's thermal balance. This article uses empirical formulas to calculate the heat carried away by engine exhaust. The specific calculation formula is as follows:

$$Q_g = M_g C_{g,p} (t_4 - t_3) \quad (6)$$

In Equation (6), M_g is the mass flow rate of the engine exhaust, kg/s; $C_{g,p}$ is the specific heat capacity of the engine exhaust at constant pressure, kJ/(kg·K); t_3 and t_4 are the intake and exhaust temperatures of the engine, respectively, K.

According to the law of conservation of mass, it can be inferred that the mass flow rate M_g of the engine exhaust should be equal to the sum of the engine intake mass flow rate and the fuel mass flow rate. The calculation formula is as follows [30].

$$M_g = M_f + M_{g,in} \quad (7)$$

$$M_f = \frac{B_e}{3600} \quad (8)$$

$$M_{g,in} = \frac{\rho_a \cdot Pr^{0.714} \cdot i \cdot V_{eb} \cdot N_e}{60 \times 2} \quad (9)$$

In Equation (9), M_f and $M_{g,in}$ are the mass flow rates of engine fuel and intake air, respectively, kg/s; ρ_a are the air density, kg/m³; Pr is the compression ratio; i is the number of cylinders, the value is 4; N_e is the volume of a single cylinder, m³.

The empirical formula for the specific heat capacity of engine exhaust at constant pressure is as follows [31]:

$$C_{g,p} = k_0 + k_1 T + k_2 T^2 + k_3 T^3 + k_4 T^4 \quad (10)$$

In Equation (10), k_0 , k_1 , k_2 , k_3 , and k_4 are the mass fractions of each exhaust gas; T is the reference temperature, K.

(5) Other heat losses of the engine Q_{other} :

The other heat losses of the engine mainly include heat dissipation from the oil pan, heat dissipation from the oil radiator, engine friction losses, etc.

3.2. Engine Cooling System Model

During engine operation, a portion of the thermal energy produced from fuel combustion is utilized to power the vehicle, while another segment is expelled into the atmosphere with the exhaust gases, and yet another is removed via the engine cooling system. The thermal energy extracted by the coolant is initially transferred to the engine cylinder block and subsequently to the engine's cooling water jacket. The high-temperature coolant within the water jacket is circulated by the water pump. When the temperature exceeds optimal levels, the thermostat regulates the coolant flow through the radiator for effective heat dissipation, thereby ensuring that the engine coolant temperature remains within a suitable range. The fluctuation in engine temperature is directly linked to the heat dissipation efficiency of the radiator. The amount of heat removed by the air during stable engine operation is equivalent to the heat extracted by the coolant flowing through the radiator. The relationship can be expressed through the following formula:

$$Q_w = V_l * \Delta T_l * \rho_l * c_l \quad (11)$$

In Equation (11), V_l is the coolant circulation rate, m³/h; ΔT_l is the temperature difference of the coolant, K; ρ_l is the engine coolant density, taken as 1074 kg/m³; c_l is the specific heat of the engine coolant, which is taken as 3.281 kJ/(kg·K).

The heat carried away by the cooling air is approximately equal to the heat lost by the coolant. The formula for the amount of cooling air is as follows:

$$Q_w = V_a * \Delta T_a * \rho_a * c_a \quad (12)$$

In Equation (12), ΔT_a is the temperature difference between the inlet and outlet air of the radiator, K; ρ_a is air density, the value is 1.01 kg/m³; c_a is the specific heat capacity of air at constant pressure, which is taken as 1.047 kJ/(kg·K). The cooling air volume can be calculated from the windward area of the radiator S_a :

$$V_a = S_a * v_a \quad (13)$$

In Equation (13), v_a is the airflow velocity in front of the engine radiator, m/s. The heat carried away by the cooling air in the engine radiator is related to the heat exchange area of the radiator, and the air volume provided by the cooling fan also has a significant impact on this heat. Based on the parameters of the radiator and cooling fan, combined with experiments, the relationship between different air flow rates and coolant flow rates of the radiator and its heat dissipation capacity is shown in Figure 4.

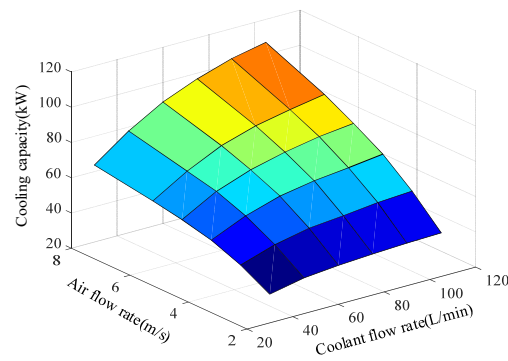


Figure 4. The relationship between the cooling capacity function, the coolant flow rate, and the airflow rate.

3.3. Engine Fuel Consumption Model

The engine's fuel consumption rate is influenced not only by the operating conditions but also by the temperature of the coolant. When determining the true fuel consumption of the engine, it is essential to apply a correction factor to the fuel consumption data, which is derived through the interpolation of engine speed and torque within the fuel consumption MAP. The formula used to calculate the engine's actual fuel consumption W_f , is articulated as follows:

$$W_f = b_e \cdot f_{cof}(t) \quad (14)$$

In Equation (14), W_f denotes the actual fuel consumption of the engine, g/kWh, while t represents the engine coolant temperature, °C. The task involves interpolating the fuel consumption correction factor in relation to the engine coolant temperature. As illustrated in Figure 5, a correlation exists between the coolant temperature and the fuel consumption correction coefficient. The graph indicates that within the coolant temperature range of 0–60 °C, there is a pronounced effect on the engine's fuel consumption correction coefficient. Furthermore, it shows that as the coolant temperature rises, the fuel consumption correction coefficient consistently decreases until it stabilizes at a value of 1.

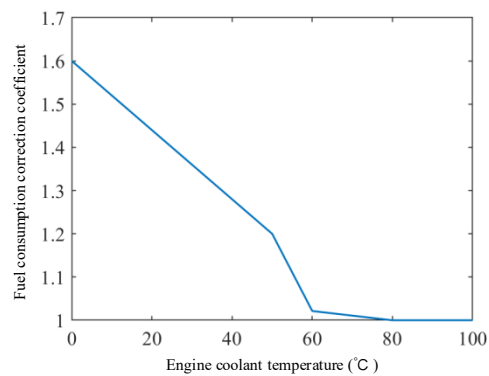


Figure 5. Engine fuel consumption correction coefficient.

3.4. Control Strategy Model

The division of operating modes for the engine waste heat recovery system mainly considers the different heating methods during engine warm-up. Specifically, it includes the following four modes: (1) cold start (the engine is heated by its own heat); (2) heat exchanger heating (the engine is heated by utilizing exhaust heat through a heat exchanger); (3) thermal battery heating (the engine is heated by the stored heat in the thermal battery); and (4) thermal battery + heat exchanger heating (the engine is heated by both exhaust heat and the stored heat in the thermal battery).

The switch between heating modes is primarily determined based on a comprehensive assessment of the engine coolant temperature and thermal battery temperature. This is

achieved by controlling the throttle valve and the three-way valve of the exhaust heat exchanger in the control loop. The control strategy for the engine waste heat recovery system is illustrated in Figure 6.

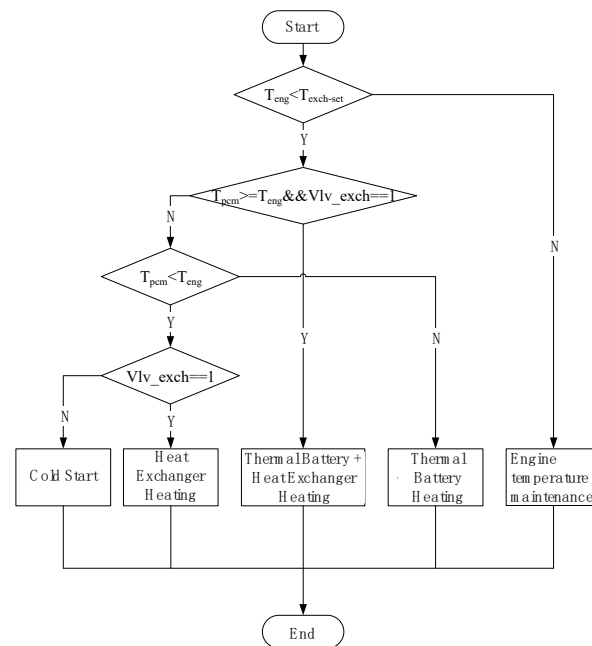


Figure 6. Control logic flowchart of engine warm-up and heating mode.

First, determine whether the engine coolant temperature T_{eng} is lower than the heat exchanger's set temperature $T_{exch-set}$ ($80\text{ }^{\circ}\text{C}$). If this condition is met and T_{pcm} is higher than T_{eng} , the three-way valve of the heat exchanger, Vlv-exch, is closed, valve RV1 is closed, valve RV2 is opened, and the system enters the thermal battery heating mode. If T_{pcm} is lower than T_{eng} , the three-way valve, Vlv-exch, is opened, valve RV1 is opened, valve RV2 is closed, and the system enters the heat exchanger heating mode. When the engine coolant temperature T_{eng} is lower than both the thermal reservoir temperature T_{pcm} and the heat exchanger's set temperature $T_{exch-set}$, the three-way valve Vlv-exch, valve RV1, and valve RV2 are all opened, and the system enters the thermal battery + heat exchanger heating mode. Otherwise, the system defaults to the cold start mode.

4. Construction and Verification of Thermal Management Simulation Platform

In accordance with the structural principles governing the engine's exhaust heat recovery system, the model developed using AMESim software 2021.1 is depicted in Figure 7. This model primarily comprises the dynamics module, the engine cooling system module, the exhaust heat exchange module, and the thermal battery module.

Both the exhaust heat exchange module and the thermal battery module are engineered to capture and repurpose the waste heat produced during engine operation. The engine cooling system module is primarily constituted of an engine water jacket, a water pump, a thermostat, an engine radiator, and a cooling fan. When modeling the engine's water jacket, it is categorized into a cylinder block water jacket and a cylinder head water jacket. The engine water pump operates mechanically and is directly connected to the engine, with its speed correlating directly to the engine's rotational speed. The engine radiator features a tubular design, incorporating cooling flat tubes and heat dissipation belts arranged longitudinally at intervals. Additionally, a cooling fan is positioned behind the radiator; this fan activates for forced heat dissipation when the engine coolant temperature exceeds optimal levels. The thermostat functions chiefly to regulate the flow of engine coolant into both the small circulation loop and the larger circulation loop that traverses the radiator. Both the exhaust heat exchange devices and thermal batteries incorporate water jackets

linked to the small circulation loop of the cooling system to elevate the temperature of the engine coolant.

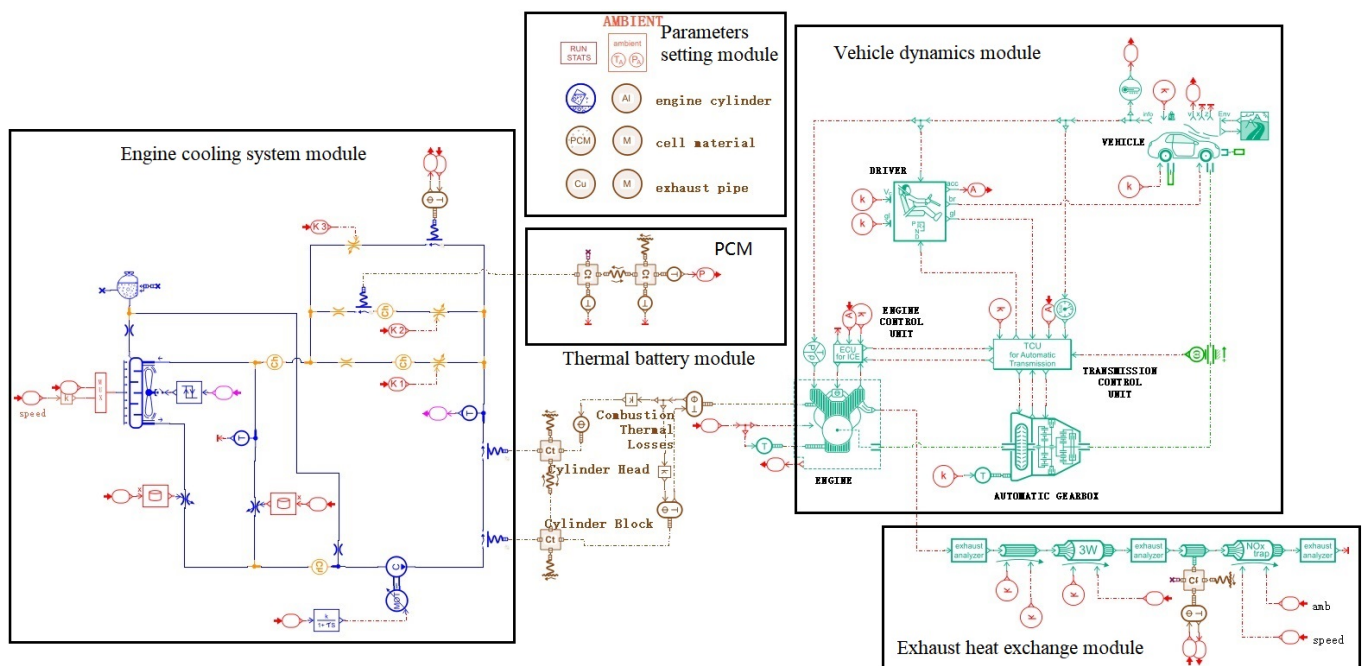


Figure 7. Simulation model of engine cooling system based on thermal battery.

The exhaust heat exchange module encompasses exhaust pipes, three-way catalytic converters, exhaust heat exchange pipes, mass blocks for exhaust heat exchange tubes, water jackets for exhaust heat exchangers, and NO_x post-processing units. Notably, the exhaust gas heat exchanger is designed in a sleeve configuration and is strategically placed downstream of the three-way catalyst to maintain catalytic efficiency. The coolant circulating within the water jacket of the exhaust heat exchanger absorbs heat from the engine exhaust and is integrated into the engine's small circulation circuit for heating purposes.

The thermal battery module consists primarily of mass blocks of PCMs, heat exchangers, and sleeves for heat exchange. Thermal exchange transpires between the PCM mass block and the heat exchanger mass block. Subsequently, the heat exchanger transfers heat to the PCM heat exchange jacket, thereby facilitating the transfer of heat from the cooling fluid in the jacket to the PCM for heat storage. Additionally, it allows for the release of stored heat from the PCM back to the cooling fluid in the heat exchange jacket.

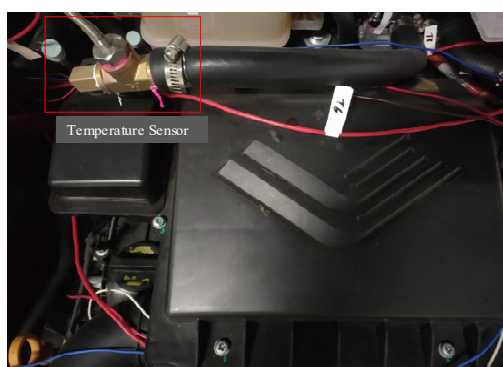
The system's thermal resistance mainly includes the thermal resistance from exhaust gas to coolant and the thermal resistance from coolant to PCM, and vice versa. Due to the fact that heat exchange is carried out through a heat exchanger, the main focus is on the thermal resistance of the heat exchanger. In the simulation software, the thermal resistance value is set through the thermal mass module.

The dynamics module encompasses the vehicle model, engine model, transmission model, driving model, and control model, all of which are utilized to compute the power requirements and fuel consumption of the engine in relation to varying driving conditions. The parameters relevant to the vehicle within this model are detailed in Table 2.

Table 2. Basic parameters of the vehicle.

Parameters	Values
Length × Width × Height/mm	4468 × 1802 × 1470
Curb weight/kg	1350
Wheelbase/mm	2620
Rolling resistance coefficient	0.014
Coefficient of air resistance	0.35
Vehicle frontal area/m ²	3.17
Wheel rolling radius/mm	379

Since this paper primarily focuses on the heat storage of the thermal battery and its role in heating the engine, the accuracy of the engine thermal model is directly related to the precision of the simulation results. To validate the precision of the engine cooling system model, an environmental chamber temperature as low as $-20\text{ }^{\circ}\text{C}$ was chosen for the actual vehicle trials (illustrated in Figure 8), with the vehicle operating condition being WLTC. Prior to conducting the experiment, modifications to the vehicle were necessary, primarily involving the installation of a temperature sensor at the outlet of the engine's water jacket. This sensor was connected to a temperature acquisition card and a controller to facilitate real-time observation and recording of changes in engine coolant temperature post-experiment commencement. The actual installation site of the temperature sensor is depicted in Figure 9.

**Figure 8.** Dynamometer and environment chamber.**Figure 9.** Temperature sensor installation diagram.

When subjected to an ambient temperature of $-20\text{ }^{\circ}\text{C}$, the comparison between the simulation curve and the experimental curve for coolant temperature during engine warm-up is presented in Figure 10. It is evident that the experimental value of the engine outlet water temperature closely aligns with the simulated value. Throughout the warm-up phase,

the simulated engine water temperature exceeds the experimental value, with a maximum temperature differential of only 4 °C; thus, the accuracy of the engine thermal model has been validated. However, since the overall thermal model also includes the thermal battery and the corresponding pipeline models and may vary slightly under different temperature conditions and operating scenarios, there are still certain uncertainties in the simulation accuracy. Nonetheless, as a proof-of-concept study, this model remains valid.

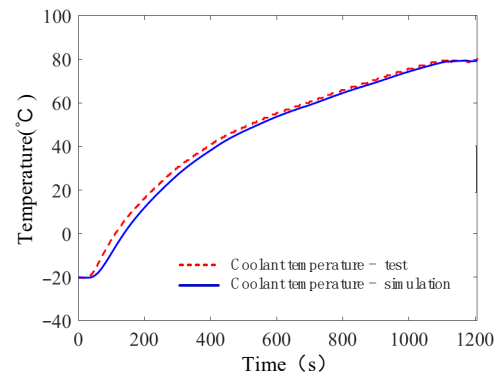


Figure 10. Simulation and experimental data of engine outlet water temperature.

5. Simulation and Analysis

5.1. Thermal Battery Performance Analysis

(1) Analysis of Thermal Storage Performance

The engine speed, torque, and heat generation of vehicles experience substantial variation under different driving conditions. With the ambient temperature set at $-20\text{ }^{\circ}\text{C}$, the vehicle was operated at consistent speeds of 40, 60, 80, and 100 km/h for a duration of 7200 s, with the average temperature variation curve of the PCM at each speed illustrated in Figure 11. The liquid phase ratio of different speeds during the heat storage process is presented in Figure 12.

From Figures 11 and 12, it is evident that during the initial phase of the simulation, the PCM remains solid across all four operating conditions, maintaining a constant temperature. As the simulation progresses, the temperature of the PCM swiftly ascends to its phase change temperature of $78\text{ }^{\circ}\text{C}$. The temperature increase initiates first under the constant speed condition of 100 km/h, followed sequentially by the conditions of 80, 60, and 40 km/h. Throughout this phase, the energy storage unit utilizes the sensible heat of the PCM for energy accumulation while the material state remains solid with a liquid phase ratio of 0. As the energy storage unit continues to absorb thermal energy, the PCM commences its melting process, causing the liquid phase ratio to progressively increase until the entire PCM transitions into a liquid state. During this transformation, the thermal battery employs the latent heat of the PCM for energy storage, resulting in a solid–liquid coexistence state of the material. Table 3 illustrates the sensible heat, latent heat, and total phase change heat storage duration of PCMs at varying vehicle speeds. For constant speeds of 60, 80, and 100 km/h, the heat storage duration decreases with an increase in vehicle speed. Notably, the total heat storage duration at a constant speed of 100 km/h amounts to 2138 s, which is 483 s shorter than the duration at a constant speed of 80 km/h, reflecting a time reduction rate of 18.42%. At 80 km/h, the total heat storage duration is recorded at 2621 s, which is 2986 s less than that at a constant speed of 60 km/h, yielding a time reduction rate of 53.25%. The latent heat storage duration necessary for a constant speed of 40 km/h is measured at 4601 s, which is less than the duration required at a constant speed of 60 km/h.

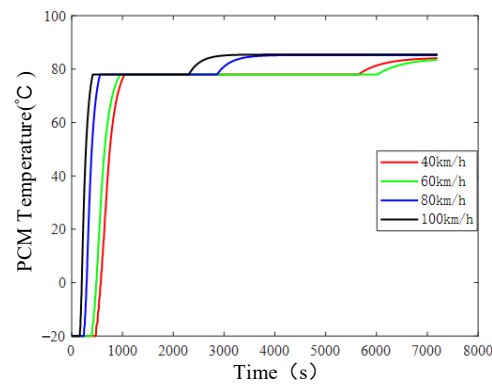


Figure 11. PCM temperature.

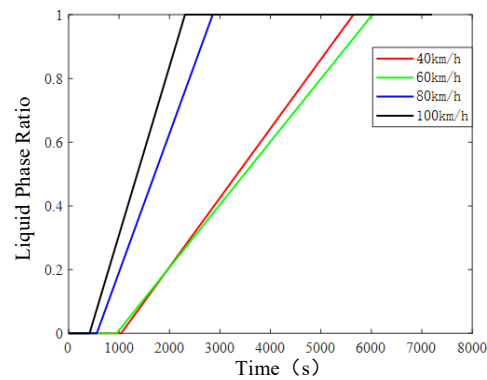


Figure 12. PCM liquid phase ratio of different speeds.

Table 3. Heat storage time of thermal battery under different speeds.

Speed/(km/h)	Sensible Heat Storage Time/s	Latent Heat Storage Time/s	Total Heat Storage Time/s
40	568	4601	5169
60	558	5044	5607
80	321	2300	2621
100	257	1881	2138

From the above, it can be concluded that within a certain range, as the driving speed increases, the engine speed also increases, resulting in a shorter time for phase change heat storage. However, when the engine speed reaches a certain limit, the effect of continuing to increase the shortening of the phase change heat storage time becomes less significant.

In examining the thermal storage capabilities of a thermal battery during high-speed operation, we have chosen to investigate the impact of ambient temperature on thermal storage performance at a constant velocity of 100 km/h. The primary operational scenarios for thermal batteries typically occur under low and normal ambient conditions. Consequently, this section selects five ambient temperatures of -20 , -10 , 0 , 10 , and 20 °C for the simulation. Following one hour of driving, the temperature variation curve of the PCMs is illustrated in Figure 13, alongside the liquid phase ratio of different initial temperatures presented in Figure 14.

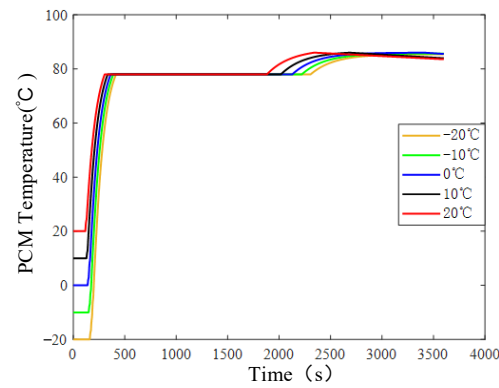


Figure 13. PCM temperature variation.

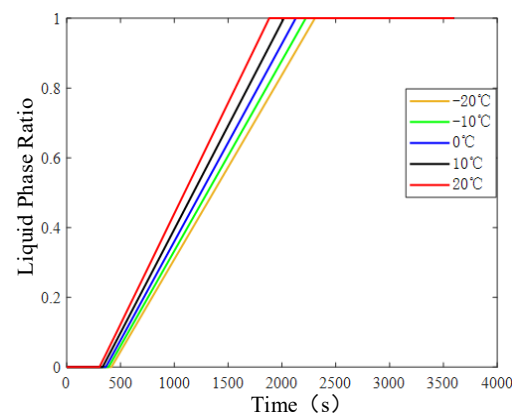


Figure 14. PCM liquid phase ratio of different initial temperatures.

Analysis of Figures 13 and 14 reveals that across the five ambient temperatures, phase change heat storage transitions through phases of sensible heat storage and latent heat storage, with the heat storage rate during the sensible heat phase significantly surpassing that of the latent phase. During the sensible heat storage phase of solid-state PCMs, the rate of temperature increase remains relatively uniform. At an ambient temperature of 20 °C, the sensible heat storage is completed first, with completion times extending inversely with decreasing ambient temperature. Throughout this phase, the liquid phase ratio of the PCM remains zero. Upon the conclusion of the sensible heat storage phase, the PCM initiates melting, leading to a gradual increase in the liquid phase ratio. Notably, the rate of increase in the liquid phase ratio is slowest at $-20\text{ }^{\circ}\text{C}$ and fastest at $20\text{ }^{\circ}\text{C}$. Table 4 summarizes the thermal storage durations of thermal batteries at varying ambient temperatures, indicating that as the ambient temperature rises, the durations for solid-state sensible heat storage, latent heat storage, and total thermal storage all diminish. Specifically, the latent heat storage duration at $-20\text{ }^{\circ}\text{C}$ is 1890 s, whereas, at $20\text{ }^{\circ}\text{C}$, it reduces to 1575 s, resulting in a time saving of 315 s, equating to a 16.67% reduction in storage duration.

Table 4. Heat storage time of thermal battery at different ambient temperatures.

Ambient Temperature/ $^{\circ}\text{C}$	Sensible Heat Storage Time/s	Latent Heat Storage Time/s	Total Heat Storage Time/s
-20	257	1890	2147
-10	243	1829	2072
0	227	1762	1989
10	207	1682	1889
20	191	1575	1766

Under varying ambient temperature scenarios, the duration of latent heat storage in PCMs fluctuates, with higher environmental temperatures correlating to shorter storage periods. This disparity primarily arises from the heat dissipation impacts stemming from both the thermal battery and the engine's interaction with the surroundings. As ambient temperatures escalate, the thermal gradient between the phase change medium and the engine diminishes, leading to a reduction in heat losses. Consequently, more energy is directed towards heating the coolant and being sequestered within the energy storage facility, thereby minimizing the duration required for phase change energy storage.

(2) Examination of Thermal Release Dynamics

In the process of thermal release from the thermal battery, both the latent heat of phase transition and the specific heat of the solid-state materials are predominantly utilized. This study assumes that the phase change medium conveys heat to precondition the engine coolant following the latent heat retention phase. The thermal release efficacy within the thermal battery is influenced by various parameters, principally the coolant's flow rate within the storage apparatus and the ambient temperature. The subsequent simulation outcomes will be derived by establishing coolant flow rates of 4, 6, 8, and 10 L/min, analyzed under low-temperature conditions of $-20\text{ }^{\circ}\text{C}$ and $0\text{ }^{\circ}\text{C}$. Figures 15–17 illustrate the temperature variations of the engine coolant and PCMs, as well as the liquid phase ratios of the phase change media across different thermal conditions, respectively.

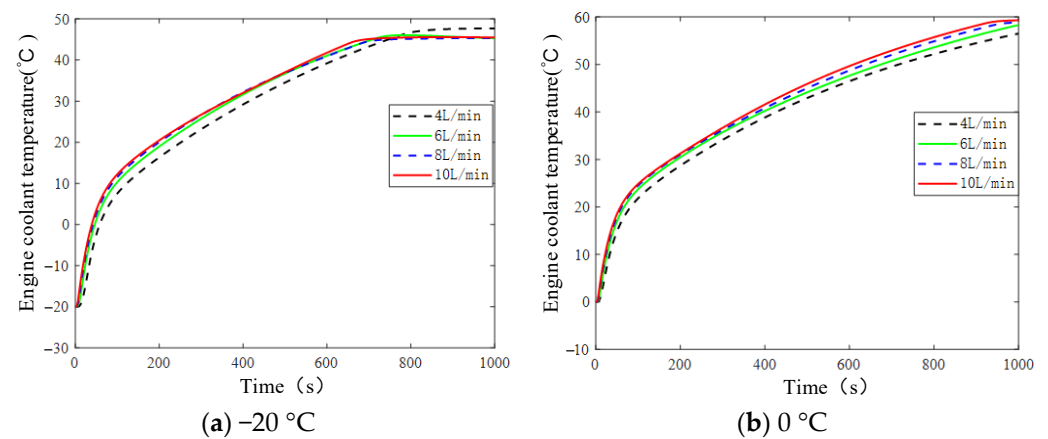


Figure 15. Temperature variation of engine coolant.

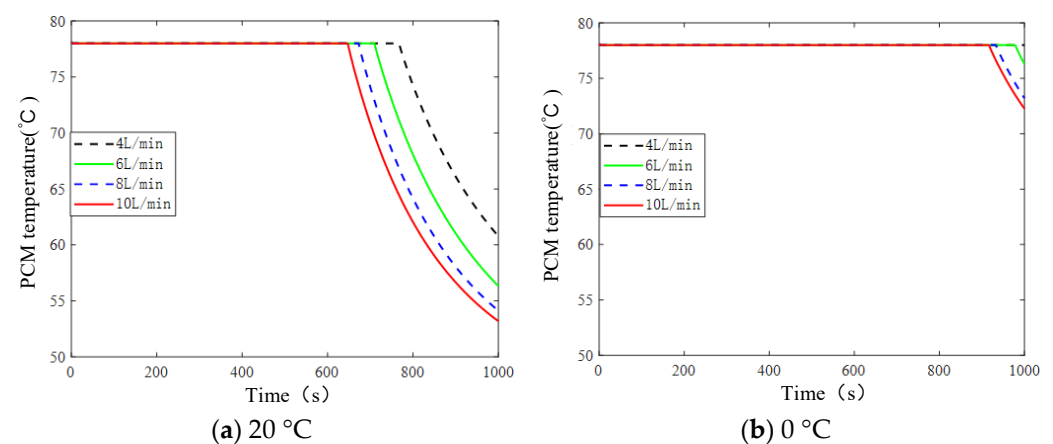


Figure 16. Temperature variation of heat release from PCMs at different temperatures.

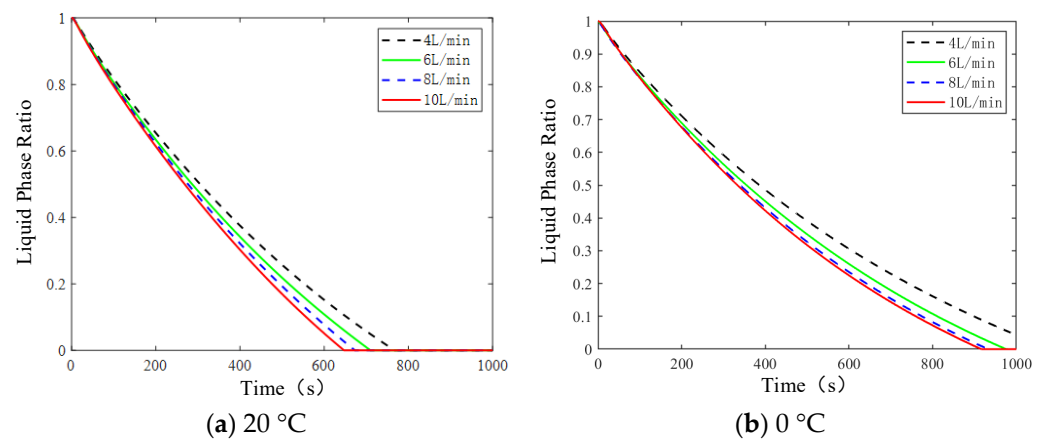


Figure 17. Liquid phase rate of heat release from PCMs.

As illustrated in the diagram, the engine coolant is preheated utilizing a thermal battery at an ambient temperature of $-20\text{ }^{\circ}\text{C}$. Initially, the coolant temperature increases swiftly during the preheating phase, subsequently decreasing in rate until it stabilizes between $45\text{ }^{\circ}\text{C}$ and $50\text{ }^{\circ}\text{C}$. Meanwhile, the PCM maintains a constant temperature of $78\text{ }^{\circ}\text{C}$ during the initial phase of latent heat release, with its liquid phase ratio gradually diminishing from 1 to 0. Throughout this process, the PCM exists in a solid–liquid coexistence state. Once the latent heat is released, the temperature of the PCM gradually declines from $78\text{ }^{\circ}\text{C}$, maintaining a liquid phase ratio of 0, indicating a solid state. The temperature variation of the engine coolant at an ambient temperature of $0\text{ }^{\circ}\text{C}$ closely parallels that observed at $-20\text{ }^{\circ}\text{C}$, with the final coolant preheating temperature ranging between 56 and $60\text{ }^{\circ}\text{C}$. The PCM persists at $78\text{ }^{\circ}\text{C}$ during the latent heat release phase, subsequently tapering down after the completion of heat release. The sensible heat from the solid PCM contributes further to the heating of the engine coolant. Notably, when the cooling liquid flow rate through the hot pool is 4 L/min , the latent heat is utilized for heat release over a simulation period of 1000 s , during which the PCM’s temperature remains constant. In contrast, under the other three flow conditions, the latent heat of the hot pool is released within the 1000-s timeframe.

At ambient temperatures of $-20\text{ }^{\circ}\text{C}$ and $0\text{ }^{\circ}\text{C}$, an increase in the coolant flow rate entering the thermal battery leads to an accelerated rate of latent heat release from PCMs, resulting in a more rapid rise in engine coolant temperature. Table 5 presents the time required for the engine coolant to reach $30\text{ }^{\circ}\text{C}$ at various flow rates. It is evident from the table that at $-20\text{ }^{\circ}\text{C}$, the time taken for the coolant to heat up is 415 s at a flow rate of 4 L/min and 371 , 361 , and 359 s at flow rates of 6 , 8 , and 10 L/min , respectively. Beyond the flow rate of 6 L/min , the improvement in heating rate is marginal; a similar trend is observed at $0\text{ }^{\circ}\text{C}$ ambient temperature, where the enhancement in heating rate due to increased coolant flow is more notable compared to $-20\text{ }^{\circ}\text{C}$ ambient temperature. This phenomenon can be attributed to the fact that an increased coolant flow rate diminishes the thermal resistance of the heat exchange between the PCM and the coolant, although there is a limit to the reduction in thermal resistance. Once the coolant flow rate surpasses a specific threshold, further increases can significantly diminish the effect of lowering thermal resistance. Initially, during heat transfer in the thermal battery, the substantial temperature difference between the PCM and the coolant amplifies the impact of varying coolant flow rates on the temperature rise rate. Consequently, as the flow rate into the thermal battery increases, the decrease in heating time fluctuates more sharply at an ambient temperature of $0\text{ }^{\circ}\text{C}$ compared to $-20\text{ }^{\circ}\text{C}$.

Table 5. The time of engine coolant heating up at different flow rates.

Environmental Temperature/ $^{\circ}$ C	Cooling Liquid Flow Rate/(L/min)	Time of the Cooling Liquid Rises to 30° C/s	Reduction Rate of Heating Time with a Flow Rate Increase of 2 L/min/%
−20	4	415	-
	6	371	10.6
	8	361	2.7
	10	359	0.554
0	4	223	—
	6	192	13.9
	8	182	5.21
	10	178	2.2

Based on the preceding data analysis, it is determined that adopting a coolant flow rate of 6 L/min for preheating the engine coolant within the thermal battery is the most suitable choice. This flow rate notably contributes to reducing the coolant temperature rise time while also ensuring lower power consumption compared to flow rates of 8 L/min and 10 L/min.

Based on the above, it can be found that the COP of the system is related to the efficiency of heat storage and release. Therefore, from the simulation data, it can be seen that when the vehicle speed is high, the heat storage is faster, and the corresponding heat loss will be relatively small. During the heat release process, the faster the coolant flow rate, the better. A moderate flow rate can bring better system efficiency.

5.2. Simulation Analysis of Engine Warm-Up Time

The rate at which the coolant temperature ascends during the engine’s cold start warm-up process significantly influences how swiftly it achieves stable operating conditions, ultimately leading to reduced fuel consumption. This study simulates four indicative operating conditions: WLTC, NEDC, 40 km/h, and 80 km/h. These are all within a low-temperature environment of -20° C. The simulation results for the engine coolant temperature rise under four cold start heating modes—thermal battery heating, exhaust heat exchanger heating, and the combined heating of both the thermal battery and heat exchanger—are presented in Figure 18. Table 6 delineates the warm-up duration of the engine coolant across different heating methods under each simulation scenario.

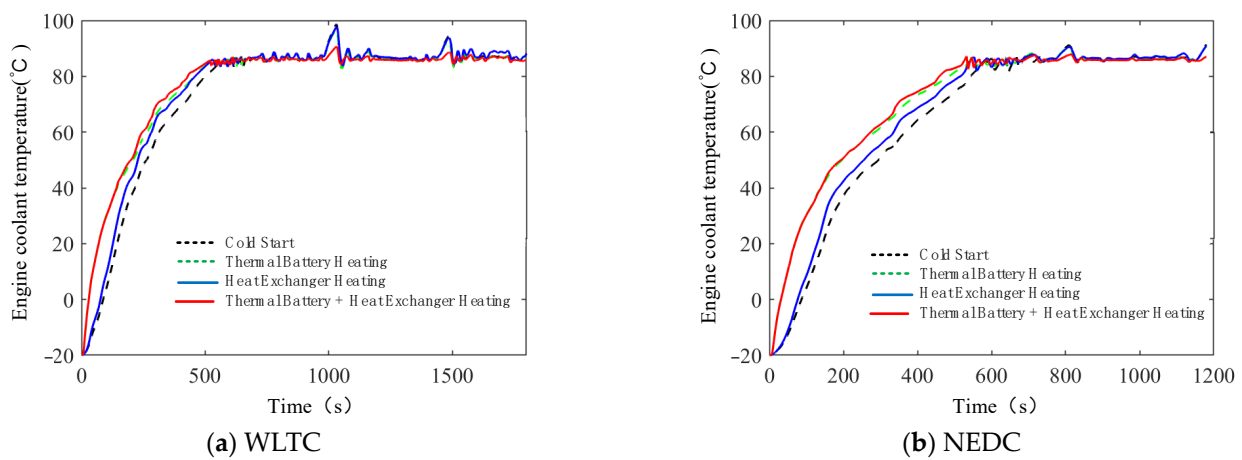


Figure 18. Cont.

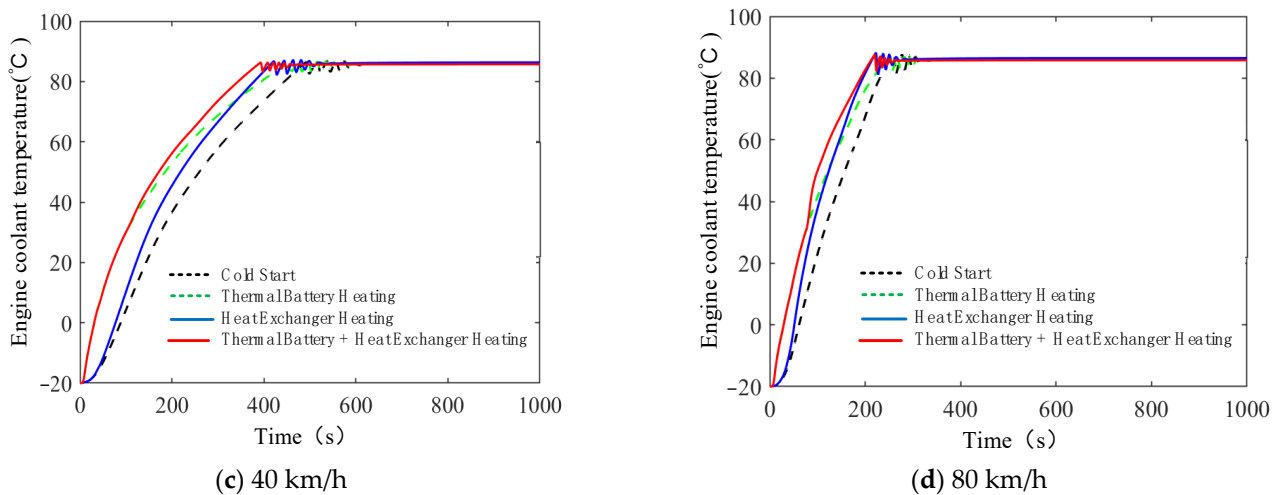


Figure 18. Engine coolant temperature under different driving conditions.

Table 6. The time for engine warm-up under different driving conditions.

Heating Mode	Engine Warm Up Time/s			
	WLTC	NEDC	40 km/h	80 km/h
Cold start	501	543	444	231
Thermal battery heating	456	475	394	216
Heat exchanger heating	460	528	378	195
Thermal battery + Heat exchanger heating	430	464	344	190

It is evident that throughout the engine warm-up under these diverse operating conditions, the coolant temperature exhibits the slowest increase during the cold start mode, requiring the longest duration to reach 80 °C. Under WLTC conditions, the warm-up period for exhaust heat exchanger heating exceeds that of thermal battery heating for the engine coolant. Conversely, under NEDC and constant speed conditions of 40 km/h and 80 km/h, the warm-up duration for the exhaust heat exchanger is shorter than that for the thermal battery. In the thermal battery heating mode, the engine coolant temperature rises rapidly at the onset when the coolant temperature is low, exhibiting a substantial temperature differential from the cold start mode. As the coolant temperature elevates, the temperature differential diminishes gradually. In contrast, during heat exchanger heating, the coolant temperature initially rises slowly, displaying a minor temperature difference compared to the cold start mode; this difference increases as the coolant temperature climbs.

Notably, when combining the thermal battery with the exhaust heat exchanger heating method, the engine coolant temperature increases most rapidly, resulting in the shortest warm-up time. This approach saves 71 s and 79 s of warm-up time compared to the engine cold start mode under WLTC and NEDC conditions, achieving time savings of 14.17% and 14.55%, respectively. For constant speed conditions of 40 km/h and 80 km/h, the time savings are 100 s and 41 s when compared to the engine cold start mode, equating to reductions of 22.52% and 17.75%, respectively.

In the thermal battery heating mode, the engine coolant experiences rapid heating during the initial phase, resulting in a larger temperature differential compared to the cold start mode. This phenomenon occurs primarily due to the significant temperature disparity between the PCM and the engine coolant at the onset of the engine warm-up, leading to a high rate of convective heat transfer, which accelerates the coolant's temperature rise. As the coolant's temperature progressively increases, the temperature differential with the PCM diminishes, consequently reducing the heating rate of the coolant.

In the heat exchanger heating mode, the exhaust gas temperature remains relatively low at the beginning, shortly after engine start, resulting in minimal convective heat transfer between the exhaust gases and the engine coolant. This slow thermal exchange leads to a modest rise in coolant temperature, yielding a smaller temperature differential in the early stages, particularly compared to the cold start mode. However, as the vehicle continues to operate, the engine exhaust temperature gradually escalates, enhancing the convective heat exchange and accelerating the coolant's temperature rise.

When integrating the thermal battery and exhaust heat exchanger in the heating mode, the thermal battery initially provides separate heating. Once the engine coolant reaches the predetermined temperature of 30 °C, the system transitions to heating via the exhaust heat exchanger. Throughout the warm-up phase, the coolant heats up relatively quickly, establishing a significant temperature differential when juxtaposed with the cold start mode.

Under constant speed conditions, the potential time savings of utilizing the combined heating mode of the thermal battery with the exhaust heat exchanger diminishes as vehicle speed increases. This trend is attributed to the escalated heat production from the engine, which results in greater heat dissipation into the cooling system, thereby weakening the influence of external devices on coolant heating.

In conclusion, of the four-engine warm-up heating modes, the thermal battery combined with the heat exchanger heating mode proves to be the most effective in minimizing warm-up time, achieving a maximum time savings rate of 22.52% at a constant speed of 40 km/h.

5.3. Fuel Consumption Analysis of Engine Cold Start and Warm-Up

The cumulative fuel consumption curves and graphs for the four-engine warm-up heating modes are presented below. Figure 19 illustrates the variations in cumulative fuel consumption of the engine during the initial 300 s under different driving scenarios. Table 7 details the cumulative fuel consumption of the engine for the first 300 s following the WLTC, NEDC, and a constant speed of 40 km/h. Table 8 presents the cumulative fuel consumption of the engine for the first 300 s at a constant speed of 80 km/h.

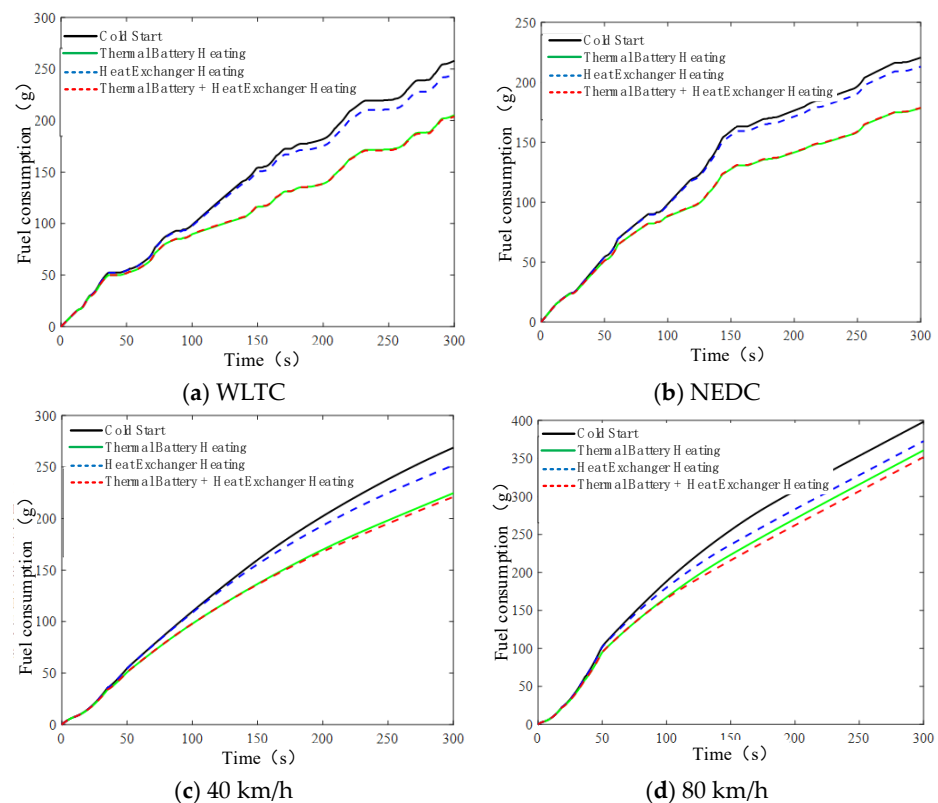


Figure 19. Fuel consumption curves in the first 300 s.

Table 7. Accumulated fuel consumption in the first 300 s.

Heating Mode	Accumulated Fuel Consumption of 300 s/g		
	WLTC	NEDC	40 km/h
Cold start	258	221	269
Thermal battery heating	205	179	225
Heat exchanger heating	245	213	251
Thermal battery + Heat exchanger heating	204	179	221

Table 8. Accumulated fuel consumption during engine warm-up of 80 km/h.

Heating Mode	Accumulated Fuel Consumption during Warm-Up/g
Cold start	336
Thermal battery heating	285
Heat exchanger heating	279
Thermal battery + Heat exchanger heating	253

It can be concluded that, under WLTC and NEDC operating conditions, the cumulative fuel consumption during the initial 70 s of exhaust heat exchanger heating closely resembles that observed during cold start mode. The cumulative fuel consumption from 70 s to 300 s is lower than that during cold start mode, albeit with a minor difference. After 300 s of operation, the cumulative fuel consumption during heat exchanger heating under WLTC and NEDC conditions shows reductions of 13 g and 8 g, respectively, translating to fuel savings of 5.04% and 3.62%. In the scenario of combining thermal battery heating and the thermal battery with exhaust heat exchanger heating, the engine's cumulative fuel consumption during the initial 70 s aligns with that in cold start mode; however, from 70 s to 300 s, the cumulative fuel consumption markedly decreases compared to cold start mode, resulting in significant fuel savings. Specifically, under WLTC and NEDC conditions, the cumulative fuel consumption during the first 300 s of the thermal battery combined with heat exchanger heating mode was recorded at 204 g and 179 g, respectively, leading to savings of 54 g and 42 g of fuel compared to the cold start mode, with fuel consumption savings of 20.9% and 19%, respectively. At a constant speed of 40 km/h, cumulative fuel consumption in the initial 300 s of thermal battery combined with heat exchanger heating mode stood at 269 g, which is 48 g less than that of the cold start mode, achieving a fuel savings rate of 17.84%. Conversely, at a constant speed of 80 km/h during engine warm-up, the cumulative fuel consumption for the thermal battery combined with heat exchanger heating mode was recorded at 253 g, indicating a reduction of 83 g compared to cold start mode, resulting in a fuel savings rate of 24.7%.

In the initial 300 s of an engine's cold start warm-up, the impact of the exhaust heat exchanger heating mode on cumulative fuel consumption is less pronounced compared to the cold start mode. This is primarily due to the lower exhaust temperature during the early warm-up phase, leading to reduced heat exchange efficiency of the exhaust heat exchanger. The temperature differential between the two heating modes at this stage is minimal; thus, the effect on fuel consumption reduction is insignificant. As the coolant temperature rises, its influence on engine fuel consumption gradually diminishes. Consequently, the heat exchanger heating mode has a marginal effect on fuel consumption during the first 300 s of warm-up when contrasted with the cold start mode. In both thermal battery heating and thermal battery combined heat exchanger heating modes, the heating effect on the coolant is notably superior during the early phase when the engine coolant temperature is low, and the impact on fuel consumption increases as the coolant temperature decreases. Thus, the fuel-saving benefits of thermal battery heating and the thermal battery combined heat exchanger heating modes significantly outperform those of the exhaust gas heat exchanger heating mode.

To summarize, among the four-engine warm-up heating strategies, the thermal battery combined with heat exchanger heating mode demonstrates the most effective reduction in engine fuel consumption. At a constant speed of 80 km/h, the fuel consumption savings rate at the conclusion of the warm-up phase peaks at 24.7%.

6. Conclusions

In conclusion, to optimize the utilization of exhaust heat from engine vehicles and enhance energy efficiency, this paper presents a design for an engine waste heat recovery thermal management system utilizing thermal battery technology. Initially, we introduced the structural principles of the thermal management system and conducted a design analysis of the thermal battery system. Following that, we analyzed the underlying principles of the engine thermal system and developed a simulation model of the vehicle thermal management system using AMESim software. The model's accuracy was validated through idle warm-up testing conditions.

Ultimately, we outlined four operational modes for engine warm-up heating and formulated control strategies for transitioning among these modes. Furthermore, we examined the factors influencing heat storage and release within the thermal battery. The findings indicated that increasing the flow rate of the cooling liquid through the thermal battery enhances the efficiency of heat storage and release. However, once the flow rate surpasses a certain threshold, the heat transfer resistance between the PCM and the cooling liquid remains relatively constant, resulting in minimal impact on the thermal battery's heat release efficiency.

We simulated and analyzed the four different operational modes of engine warm-up heating under distinct operating conditions, including WLTC, NEDC, and constant speeds of 40 km/h and 80 km/h. The results highlighted that the operational mode integrating the thermal battery with the exhaust heat exchanger provided the most significant reduction in warm-up time and fuel consumption. Notably, in comparison to the cold start mode, maintaining a constant speed of 40 km/h led to the highest reduction in warm-up time, achieving a 22.52% decrease. Meanwhile, at a constant speed of 80 km/h, the greatest savings in cumulative fuel consumption were realized, totaling 24.7%.

The analysis above explores the feasibility of applying thermal battery technology to engine-powered vehicles, as well as its effects on improving cold start times and reducing energy consumption. However, one limitation is the lack of sufficient physical experimental validation, which is the focus of our next step. Moving forward, we plan to modify the thermal management loop in real vehicles and conduct tests in low-temperature environments to evaluate the actual heating performance, further validating the effectiveness of this technology.

Moreover, thermal battery technology is not limited to engine-powered vehicles. It can have an even more significant impact on hybrid vehicles. The stored thermal energy can not only reduce engine warm-up time during cold starts but also heat the battery and cabin, significantly improving overall vehicle comfort during start-up. Additionally, during driving, it can supply heat while the engine is off, substantially reducing overall vehicle energy consumption. This area of research will also be a key focus for us moving forward. We aim to integrate thermal batteries into hybrid vehicle thermal management systems, optimizing control strategies, and conducting real-world vehicle tests. This will further validate the potential for commercial applications and the prospects of this technology.

Author Contributions: Conceptualization, B.Z.; methodology, B.Z.; software, Y.Z.; validation, Y.Z.; formal analysis, Y.Z.; investigation, D.W.; resources, D.W.; data curation, D.W.; writing—original draft preparation, B.Z.; writing—review and editing, Y.Z.; visualization.; supervision.; project administration, D.W.; funding acquisition, B.Z. All authors have read and agreed to the published version of the manuscript.

Funding: This research was funded by [Anhui Provincial Natural Science Foundation Project] grant number [2308085ME159].

Data Availability Statement: The original contributions presented in the study are included in the article, further inquiries can be directed to the corresponding authors.

Conflicts of Interest: The authors declare no conflicts of interest.

Nomenclature

COP	Coefficient of performance
EGR	Exhaust gas recirculation
EHRS	Exhaust heat recovery system
PCM	Phase change materials
NEDC	New Europe Drive Cycle
NOx	Nitrogen oxides
WLTC	World Light Vehicle Test Cycle
B_e	The fuel consumption of the engine [kg/h]
b_e	The specific fuel consumption rate of the engine [g/(kW·h)]
c_l	The specific heat of the engine coolant [kJ/(kg·K)]
c_a	The specific heat capacity of air at constant pressure [kJ/(kg·K)]
$C_{w,p}$	The constant pressure specific heat capacity of the engine coolant [kJ/(kg·K)]
$C_{g,p}$	The specific heat capacity of the engine exhaust at constant pressure [kJ/(kg·K)]
H_u	The fuel calorific value [kJ/kg]
i	The number of cylinders
k_0, k_1, k_2, k_3, k_4	The mass fractions of each exhaust gas
M_w	The mass flow rate of the coolant [kg/s]
M_g	The mass flow rate of the engine exhaust [kg/s]
M_f	The mass flow rates of engine fuel [kg/s]
$M_{g,in}$	The mass flow rates of engine intake air [kg/s]
N_e	The engine speed [r/min]
Pr	Compression ratio
Q_f	The engine total heat
Q_e	The heat converted into effective work
Q_w	The heat carried away by the engine coolant
Q_g	the heat carried away by engine exhaust
Q_{other}	The other heat losses of the engine
S_a	The windward area of the radiator
T_e	The engine torque [Nm]
t_1	The inlet water temperatures of the engine water jacket coolant [K]
t_2	The outlet water temperatures of the engine water jacket coolant [K]
t_3	The intake temperatures of the engine exhaust [K]
t_4	The outtake temperatures of the engine exhaust [K]
ΔT_a	The temperature difference between the inlet and outlet air of the radiator [K]
ΔT_l	The temperature difference of the coolant [K]
T_{eng}	The engine coolant temperature [°C]
$T_{exch-set}$	The heat exchanger's set temperature [°C]
T_{pcm}	The PCM temperature [°C]
V_l	The coolant circulation rate [m ³ /h]
v_a	The airflow velocity in front of the engine radiator [m/s]
W_f	The actual fuel consumption of the engine [g/kWh]
ρ_a	The air density [kg/m ³]
ρ_l	The engine coolant density [kg/m ³]

References

1. Wang, Q. Study on the Economic Driving Mode of Light Commercial Vehicles. Master's Thesis, Chang'an University, Xi'an, China, 2011.
2. Shi, B. Heating System Utilizing Engine Waste Heat through Heat Pipes. *Foreign Automob.* **1990**, *5*, 1–3.

3. Liu, P.; Shu, G.; Tian, H. Methodology for Achieving Optimal Practical Organic Rankine Cycle (OP-ORC) via Configuration Modifications for Diesel Engine Waste Heat Recovery. *Energy* **2019**, *174*, 543–552. [[CrossRef](#)]
4. Xu, Y.; Cui, Y.; Wang, Y.; Wang, P. Simulation Analysis of Exhaust Turbine Power Generation for Waste Heat Recovery from a Diesel Engine Exhaust. *Energy Rep.* **2021**, *7*, 8378–8389. [[CrossRef](#)]
5. Mohamed, E.S. Development and Performance Evaluation of a Thermoelectric Generator System Utilizing Exhaust Recovery for Light Diesel Vehicles, with Assessment of Fuel Economy and Emissions. *Appl. Therm. Eng.* **2019**, *147*, 661–674. [[CrossRef](#)]
6. Shen, H.; Lin, L. Research on Engine Exhaust Heat Recovery Based on the Synergistic Effect of Superconducting Heat Pipes and Thermoelectric Power Generation Technology. *Times Auto* **2020**, *15*, 141–143.
7. Li, Z. Research on Waste Heat Utilization Technology of Mining Vehicle Engines Based on the Rankine Cycle. Master's Thesis, Xijing College, Xi'an, China, 2018.
8. Ding, M. Research on Lithium Bromide Cooling System Driven by Automotive Engine Waste Heat. Master's Thesis, Zhejiang University of Science and Technology, Hangzhou, China, 2019. [[CrossRef](#)]
9. Kotrba, A.; Gardner, T.; Bellard, R.; Kunkel, B.; Morley, N.; Wang, X.; Qu, S. Solutions for Active Exhaust Waste Heat Recovery Systems. *Automot. New Power* **2021**, *4*, 12–18. [[CrossRef](#)]
10. Xie, P.; Jin, L.; Qiao, G.; Lin, C.; Barreneche, C.; Ding, Y. Thermal energy storage for electric vehicles at low temperatures: Concepts, systems, devices, and materials. *Renew. Sustain. Energy Rev.* **2022**, *160*, 112263. [[CrossRef](#)]
11. Kauranen, P.; Elonen, T.; Wikström, L.; Heikkinen, J.; Laurikko, J. Temperature Optimization of a Diesel Engine Utilizing Exhaust Gas Heat Recovery and Thermal Energy Storage (Diesel Engine with Thermal Energy Storage). *Appl. Therm. Eng.* **2010**, *30*, 631–638. [[CrossRef](#)]
12. Johar, D.K.; Sharma, D.; Soni, S.L.; Gupta, P.K.; Goyal, R. Experimental Investigation on Latent Heat Thermal Energy Storage System for Stationary CI Engine Exhaust. *Appl. Therm. Eng.* **2016**, *104*, 64–73. [[CrossRef](#)]
13. Kaltakkiran, G.; Ceviz, M.A. Performance Enhancement of Direct Injection Engines in Cold Start Conditions through Integration with Phase Change Materials: Energy and Exergy Analysis. *J. Energy Storage* **2021**, *42*, 102895. [[CrossRef](#)]
14. Soliman, A.S.; Radwan, A.; Xu, L.; Dong, J.; Cheng, P. Energy Harvesting in Diesel Engines to Mitigate Cold Start-Up Issues using Phase Change Materials. *Case Stud. Therm. Eng.* **2022**, *31*, 101807. [[CrossRef](#)]
15. Kraft, W.; Altstedde, M.K. Utilization of Metallic Phase Change Materials (mPCM) for Thermal Storage in Electric and Hybrid Vehicles. In Proceedings of the 6th Hybrid and Electric Vehicles Conference (HEVC 2016), London, UK, 2–3 November 2016.
16. Kraft, W.; Jilg, V.; Altstedde, M.K.; Lanz, T.; Schwarz, D. High-Performance Thermal Storage Solutions for Vehicle Applications. In Proceedings of the International Conference on Energy and Thermal Management, Air Conditioning, Waste Heat Recovery, Berlin, Germany, 22–23 November 2018; Springer: Berlin/Heidelberg, Germany, 2018.
17. Wang, Y.; Yu, S.; Li, J. Experimental Study on the Application of Phase Change Thermal Storage Technology to Improve Engine Cold Start Performance. *J. Sol. Energy* **2013**, *34*, 160–164.
18. Yang, Q.; Yan, J.; Liu, D. Parameter analysis of the ball-symmetric solidification process for recovering engine waste heat. *J. Agric. Mach.* **2006**, *3*, 27–30.
19. Gao, Q.; Wang, Y.; Wang, G.; Wang, Y.; Li, M.; Ma, C. Analysis of the functional characteristics based on the utilization of vehicle waste heat energy storage. *Therm. Sci. Technol.* **2008**, *7*, 314–319.
20. Hadden, T. Thermal Storage for Electric Vehicle Cabin Heating in Cold Weather Conditions. Ph.D. Thesis, McMaster University, Hamilton, ON, USA, 2017.
21. Zeng, Z.Y.; Zhao, B.C.; Wang, R.Z. Water-based adsorption thermal battery: Sorption mechanisms and applications. *Energy Storage Mater.* **2023**, *54*, 794–821. [[CrossRef](#)]
22. Zhao, H.; Dai, J.; Fu, B.; Ling, R. Design and application research of phase change thermal energy storage pools. *Sci. Enterp.* **2016**, *3*, 215–216.
23. Dreissigacker, V.; Belik, S. High-temperature solid media thermal energy storage system with high effective storage densities for flexible heat supply in electric vehicles. *Appl. Therm. Eng.* **2019**, *149*, 173–179. [[CrossRef](#)]
24. Bauer, S.; Suchanek, A.; Leon, F. Thermal and energy battery management optimization in electric vehicles using Pontryagin's maximum principle. *J. Power Sources* **2014**, *246*, 808–818. [[CrossRef](#)]
25. Behi, H.; Karimi, D.; Behi, M.; Nargesi, N.; Aminian, M.; Ghanbarpour, A.; Mirmohseni, F.; Van Mierlo, J.; Berecibar, M. An enhanced phase change material composite for electrical vehicle thermal management. *Designs* **2022**, *6*, 70. [[CrossRef](#)]
26. Xiao, Q.; Yuan, W.; Li, L.; Xu, T. Fabrication and characteristics of composite phase change material based on Ba(OH)₂·8H₂O for thermal energy storage. *Sol. Energy Mater. Sol. Cells* **2018**, *6*, 70. [[CrossRef](#)]
27. Li, Z.; Zhong, D.; Zhou, H.; Cai, Q.; Liu, Y.; Liu, L.; Ma, F. Effect of nucleating agent on the thermal storage performance of Ba(OH)₂·8H₂O as a phase change material. *Mater. Res. Express* **2019**, *9*, 095514. [[CrossRef](#)]
28. Cui, K.; Liu, L.; Sun, M. Study on improving the heat storage property of Ba(OH)₂·8H₂O with paraffin. *Mater. Res. Express* **2017**, *4*, 125502. [[CrossRef](#)]
29. Jiao, Q. Analysis of Engine Thermal Balance and Calculation of Cooling Water Thermal Utilization for Large Buses. Master's Thesis, Shandong University, Jinan, China, 2008.

30. Cui, F. Research on the Characteristics of a Dual-Heat-Source Driven Absorption-Compression Hybrid Refrigeration Cycle. Master's Thesis, Shandong University of Science and Technology, Qingdao, China, 2020.
31. Gao, C. Interactive Thermal Analysis of the Power Cabin of Range-Extended Electric Vehicles and Design of the Thermal Management System. Master's Thesis, Jilin University, Changchun, China, 2016.

Disclaimer/Publisher's Note: The statements, opinions and data contained in all publications are solely those of the individual author(s) and contributor(s) and not of MDPI and/or the editor(s). MDPI and/or the editor(s) disclaim responsibility for any injury to people or property resulting from any ideas, methods, instructions or products referred to in the content.